



Laser ablation of natural micas: Synthesis of MgO and Mg(OH)₂ nanoparticles and nanochains



V.S. Vendamani^a, Ajay Tripathi^b, Anand P. Pathak^a, S. Venugopal Rao^c, Archana Tiwari^{b,*}

^a School of Physics, University of Hyderabad, Hyderabad 500046, India

^b Department of Physics, Sikkim University, Gangtok 737102, India

^c ACRHEM, University of Hyderabad, Hyderabad 500046, India

ARTICLE INFO

Article history:

Received 26 November 2016

Received in revised form 13 January 2017

Accepted 17 January 2017

Available online 19 January 2017

Keywords:

Muscovite

Biotite

Nanoparticles

Laser processing

ABSTRACT

MgO and Mg(OH)₂ nanoparticles and nanochains are prepared by laser ablation of natural micas in water. The laser ablation of muscovite and biotite, yielded spherical nanoparticles of average diameter of 36 and 63 nm, whereas the diameter of the obtained nanochains ranged between 40 and 80 nm. The nominal lengths of the network structures are in the range of 400 nm to few microns. The synthesized nanoparticles and nanochains networks show a plasmon resonance band near the UV region.

© 2017 Elsevier B.V. All rights reserved.

1. Introduction

Laser ablation (LA) of targets in liquids is a cleaner approach to synthesize stable dispersion of nanomaterials without using chemical reagents and surfactants [1,2]. These targets have been metals, their oxides or salts dissolved in various solvents including water. Ultrashort pulsed LA yields isolated nanoparticles (NP) where the material undergoes quick non-thermal heating and extreme thermo-elastic pressure in liquid media [3].

MgO and Mg(OH)₂ NP are utilised in surface adsorption, catalysis, plasma displays, flame retardation, bactericidal effects and conservation of old papers [4–7]. In addition to these NP, LA of Mg target [8–10] also produces one dimensional nanostructures, such as nanorods and nanoneedles. However, their synthesis requires presence of surfactants, templates or precursors which are in general harmful chemicals.

Here we present first report on the novel, green and one-step synthesis of MgO and Mg(OH)₂ NP and their nanochains (NC) by LA of natural mica minerals in water. The synthesised nanosystems require no surfactants/templates for their organisation. This simple approach can be easily scaled up for mass synthesis of these NP and their NC for wide range of applications.

2. Materials and methods

XRD patterns were obtained by D8 Bruker diffractometer with CuK α radiation. Raman spectra of the pristine and ablated samples were obtained using Horiba Jobin Yvon confocal spectrometer (at 633 nm) and Reinshaw inVia spectrometer (at 785 nm) respectively. SEM (Carl Zeiss, FEG, Ultra-55), X-ray energy dispersive spectrometry (EDS) (Oxford Inca) and TEM (Technai G² S-T) were utilised to analyse surface morphology and chemical composition of the samples. UV- vis spectra were recorded using JASCO V-570 spectrophotometer.

40 fs Ti: sapphire laser system (Coherent Legend, ~2.5 W, 1 kHz) operating at 800 nm and delivering the pulse energy of ~100 μ J was used for LA of the mica targets which were placed in a Pyrex cell filled with water (5 mm above the target surface) [11]. Theoretical beam waist at the focus was nearly 30 μ m. The targets were placed normal to laser beam on a motorized X-Y stage which was controlled by an ESP 300 motion controller. The LA time was 60 min throughout the measurement.

3. Results and discussion

The elemental compositions of pristine and laser ablated muscovite and biotite are given in Table 1. In addition to the ideal composition of pristine muscovite i.e. KAl₂(AlSi₃O₁₀)(OH)₂, presence of trace elements like Mg, Fe, Cl, Cu, I, Sn and Na are observed. The

* Corresponding author.

E-mail address: archana.tiwari.ox@gmail.com (A. Tiwari).

Table 1
Elemental composition of muscovite and biotite obtained by EDS analyses.

Element	Muscovite		Biotite	
	Pristine	Ablated	Pristine	Ablated
	Weight (%)		Weight (%)	
O	28	72.4	45.8	81.4
Mg	0.5	4.8	9.3	5.1
Si	7.0	2.6	18.8	0
K	2.8	2.4	7.5	12.2
Na	0.1	6.2	0.1	1.3
Al	59.5	0	10.4	0
Fe	0.3	0	8.0	0
Cl	0.9	4.1	0	0
I	0.9	7.4	0	0
Total	100	100	100	100

composition of biotite is found to be $K(Mg,Fe^{2+}, Fe^{3+})_3(AlSi_3O_{10})(OH)_2$ with traces of Ti in it.

EDS data of laser ablated muscovite and biotite particles are also given in Table 1. The composition of muscovite and biotite particulates dissolved in water have changed significantly upon LA. Most of the elements observed in the pristine samples have been eliminated during the ablation and water dissolution processes whereas large particulates of mica are filtered during the sample characterization. Only, Mg, K and Na are observed in both laser ablated mica solutions.

XRD patterns of pristine and laser ablated muscovite and biotite are shown in Fig. 1 and are in agreement with the previous reports [12]. The patterns of laser ablated micas (Fig. 1(b and d)) show presence of both hexagonal $Mg(OH)_2$ and cubic MgO in the two samples [10,13]. Apparently, the molecular clusters produced by

LA of muscovite and biotite are dispersed in water and this is why we observed both $Mg(OH)_2$ and MgO clusters in the solution.

XRD peaks of laser ablated mica samples exhibit narrower linewidths as compared to previously synthesised MgO and $Mg(OH)_2$ NP during the LA of Mg targets [8–10]. This could be attributed to their large crystallite size. For instance, the peaks corresponding to (100) and (111) planes exhibit crystallite size of 175 and 108 nm respectively for laser ablated muscovite whereas the peaks corresponding to (111) and (200) planes exhibit crystallite size of 47 and 96 nm respectively for laser ablated biotite.

The laser-generated colloids of muscovite and biotite in water exhibit strong absorption in the region between 250 and 350 nm (See Fig. 1(e and f)). These are characteristic plasmon resonance peaks and are observed near 300 nm in MgO and $Mg(OH)_2$ NP [8]. In laser ablated muscovite, a sharp resonance is observed at 290(1) nm with a linewidth of 15(1) nm. In laser ablated biotite, the peak, observed at 290(2) nm with a linewidth of 14(2), is accompanied with a broad shoulder peak at 313(1) nm having linewidth 37(2) nm. Previous reports on LA of Mg in acetone and propanol have also found the plasmon absorption at 330.6 nm and, 230.8 and 326 nm respectively [8].

Raman spectra of pristine muscovite and biotite are shown in Fig. 2(a) and (c) respectively and are at par with those reported previously [14]. NP generated by the LA of mica targets in water are also presented in Fig. 2(b and d). The observed spectrum closely resembles to that of MgO and $Mg(OH)_2$ nanostructures [15]. Biotite NP show only one distinct Raman peak at 192 cm^{-1} which is also seen in the spectrum of the bulk target. Interestingly, most of the Raman peaks, as observed for the bulk muscovite and biotite, disappear in the laser ablated samples.

Fig. 3(a and b) illustrate SEM images of laser ablated muscovite and biotite respectively. LA of muscovite yields spherical and rod

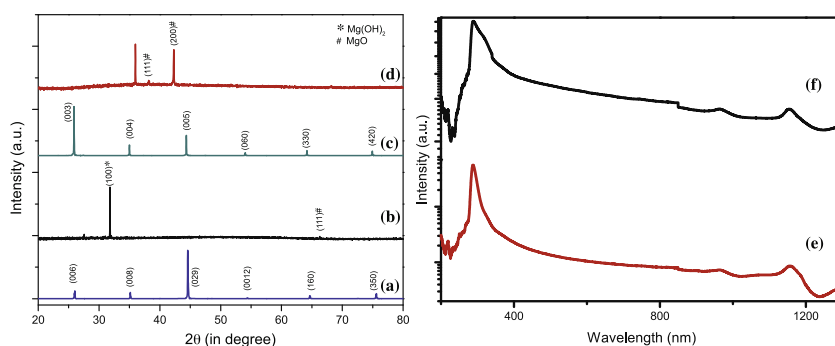


Fig. 1. XRD patterns of (a) bulk Muscovite, (b) laser ablated NP of Muscovite, (c) bulk Biotite, (d) laser ablated NP of Biotite. Absorption spectra of the ablated NP of (e) Muscovite and (f) Biotite.

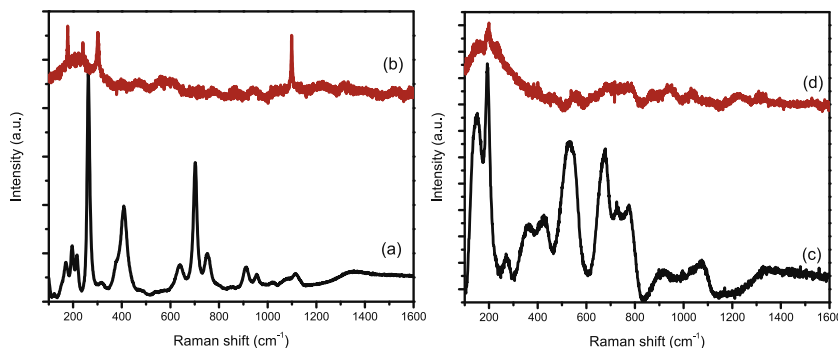


Fig. 2. Raman spectra of pristine (a) Muscovite and (c) Biotite, and laser ablated (b) Muscovite and (d) Biotite.

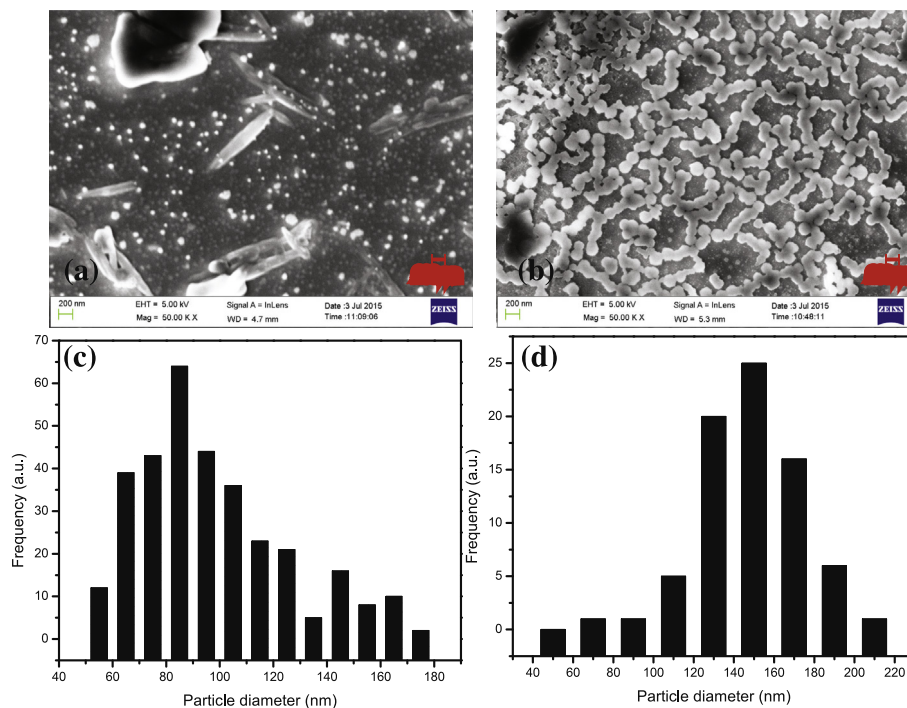


Fig. 3. SEM micrographs of NP prepared from LA of (a) Muscovite and (b) Biotite. The particle size distribution of (a) and (b) are shown in (c) and (d) respectively.

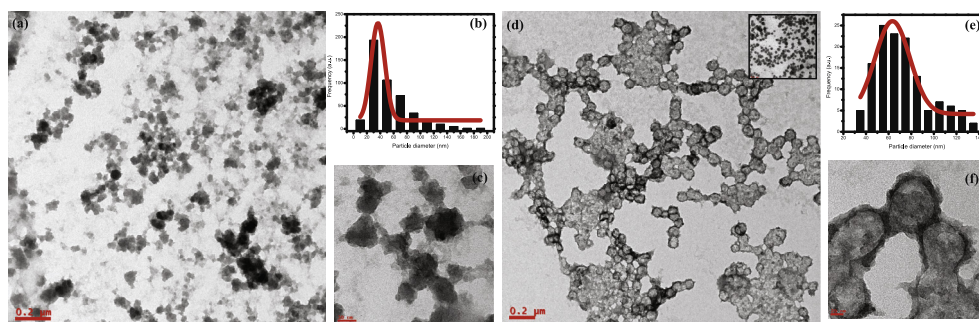


Fig. 4. TEM micrographs of NP prepared from LA of Muscovite (a, b and c) and Biotite (d, e and f).

shaped NP whose size distribution ranges between 50 and 180 nm (Fig. 3(c)). LA of biotite yields larger NP having only spherical geometry and a wider size distribution between 60 and 220 nm as shown in Fig. 3(d).

It can be noted from Fig. 3 that unlike muscovite NP, the NP of biotite are connected together, forming a large extended network with a length ranging from 400 nm to a few microns. These structures appear to be chain-like where NP are interconnected giving rise to a network like structure in water.

Fig. 4(a and c) show TEM micrographs of the muscovite NP. Fig. 4(b) shows a wide size distribution of spherical NP whose diameter range from 10 to 160 nm. The NP have an average size of 36 nm. Fig. 4(c) shows that laser ablated muscovite NP tend to agglomerate to form larger NP in water and thus giving rise to a wide size distribution.

Fig. 4(d and f) show TEM micrographs of the biotite NP. Fig. 4(e) shows a wide distribution of spherical NP whose diameter range from 30 to 140 nm. These NP exhibit an average size of 63 nm. Most of the synthesised NP tend to align themselves in a linear fashion forming chain like nanostructures with average diameter of about 50 nm. The higher magnification TEM image (Fig. 4(f)) clearly shows aligned arrangement of single NP which are inter-

connected to form an extended NC. Few recent reports on LA in liquids have shown the synthesis of nanochain like structures [16,17] where temperature, laser fluence, colloidal concentration are found responsible for their syntheses. In this study, we feel that the fluences used are high enough to promote the melting of individual NP and thereby inducing the formation of interconnected particles and their networks. However, further detailed studies are warranted to completely understand this phenomenon.

4. Conclusion

Nanostructures of MgO and Mg(OH)₂ were synthesized by ultra-short pulsed LA of muscovite and biotite targets in water. The average size of the as-synthesised NP is comparable to those prepared by chemical and hydrothermal routes. LA of muscovite yields well dispersed NP of size ranging between 10 and 160 nm whereas LA of biotite favours self-assembly of NP into nanochains of average diameter of 50 nm. LA of these readily available minerals in water provides a flexible and template-free approach for the large scale production of MgO and Mg(OH)₂ nanostructures which may find immediate applications in the field of nano-optoelectronics and

nano-photonics where highly ordered nanostructures are a prerequisite. The method is general and is extendable to other minerals enriched in Mg.

Acknowledgement

VSV and APP thank CSIR New Delhi and S V Rao thanks DRDO and UPE-II, UoH for the financial support.

References

- [1] G. Yang, *Prog. Mater. Sci.* 52 (2007) 648–698.
- [2] H. Zeng, X.-W. Du, S.C. Singh, S.A. Kulinich, S. Yang, J. He, W. Cai, *Adv. Funct. Mater.* 22 (2012) 1333–1353.
- [3] G. Yang, *Laser Ablation in Liquids: Principles and Applications in the Preparation of Nanomaterials*, CRC Press, 2012.
- [4] C. Yan, D. Xue, *J. Phys. Chem. B* 109 (2005) 12358–12361.
- [5] N.C.S. Selvam, R.T. Kumar, L.J. Kennedy, J.J. Vijaya, *J. Alloys Compd.* 509 (2011) 9809–9815.
- [6] H. Cao, H. Zheng, J. Yin, Y. Lu, S. Wu, X. Wu, B. Li, *J. Phys. Chem. C* 114 (2010) 17362–17368.
- [7] R. Giorgi, C. Bozzi, L. Dei, C. Gabbiani, B.W. Ninham, P. Baglioni, *Langmuir* 21 (2005) 8495–8501.
- [8] T.X. Phuoc, B.H. Howard, D.V. Martello, Y. Soong, M.K. Chyu, *Opt. Lasers Eng.* 46 (2008) 829–834.
- [9] C. Liang, T. Sasaki, Y. Shimizu, N. Koshizaki, *Chem. Phys. Lett.* 389 (2004) 58–63.
- [10] Z. Yan, R. Bao, C.M. Busta, D.B. Chrisey, *Nanotechnology* 22 (2011) 265610.
- [11] G.K. Podagatlapalli, S. Hamad, S.V. Rao, *J. Phys. Chem. C* 119 (2015) 16972–16983.
- [12] A. Tiwari, A. Tripathi, A.P. Pathak, *Nucl. Instrum. Methods Phys. Res., Sect. B* 343 (2015) 9–14.
- [13] S.Y. Sawant, S. Senthilkumar, R.S. Somani, M.H. Cho, H.C. Bajaj, *Mater. Lett.* 187 (2017) 72–75.
- [14] A. Tlili, D. Smith, J. Beny, H. Boyer, *Mineral. Mag.* 53 (1989) 165–179.
- [15] S. Heitz, J.-D. Epping, Y. Aksu, M. Driess, *Chem. Mater.* 22 (2010) 4563–4571.
- [16] H. He, W. Cai, Y. Lin, B. Chen, *Chem. Commun.* 46 (2010) 7223–7225.
- [17] P. Jafarkhani, M. Torkamany, S. Dadras, A. Chehrghani, J. Sabbaghzadeh, *Nanotechnology* 22 (2011) 235703.